Properties of Vacuum Phototriodes in a 4 T Magnetic Field

Christine Drown
Spring 2008
PHYS 393
Professor Hirosky

CMS Background

The Compact Muon Solenoid experiment is a general purpose detector being built for the Large Hadron Collider at CERN. Its "compact" design will weigh 12500 tons and be 21 m long and 16m in diameter. The compact in the name can be attributed to the fact that it is smaller than ATLAS, the other general purpose detector on the LHC. While ATLAS will rely on both an inner solenoid and an outer toroid to generate its magnetic field, CMS will use a superconducting solenoid magnet. Supersymmetry and the Higgs boson are just some of the physics that will hopefully be probed in this experiment.

The CMS detector is a large cylinder surrounding the proton beam which travels through its center. The detector is divided into layers as one travels out in radius, with each layer designed to accomplish different tasks. The first layer is made up of silicon detectors, allowing the particles motions to be tracked. By following their arc in response to the 4T magnetic field, their momenta may be deduced. This silicon tracker is the largest of its kind, containing 66 million pixels! Beyond the silicon tracker lies the electromagnetic calorimeter, a grouping of nearly 80,000 scintillating lead tungstate crystals, 61,200 Avalanche Photodiodes (APDs), and over 14,000 Vacuum Phototriodes (VPTs). The APDs were selected for their high gain. However, the APDs are not radiation-hard enough for placement near the endcaps of the detector where the radiation dose (primarily of concern are neutrons) over time is expected to be too large for the APDs to function reliably. Here, VPTs are used instead. VPTs are sufficiently rad-hard for the task and maintain operation under high magnetic fields; however, VPTs' gains do not remain fixed with time, but rather fluctuate depending on the recency and strength of the input light. It is this instability of the gain that makes VPTs difficult to calibrate (and thus calorimetry difficult to accomplish), and that will be the primary focus of this paper. Following the electromagnetic calorimeter is the hadron calorimeter, composed primarily of dense brass and steel which act to create hadron showers. The showers are then detected by plastic scintillators. The final layer of the CMS detector, the muon detector, sits outside the superconducting magnet. To counteract this, an iron return yoke is layered with muon chambers. This allows momentum measurements to be made on muons. yokes are put in place to See Figure 1 for a schematic of the layers of the CMS detector.

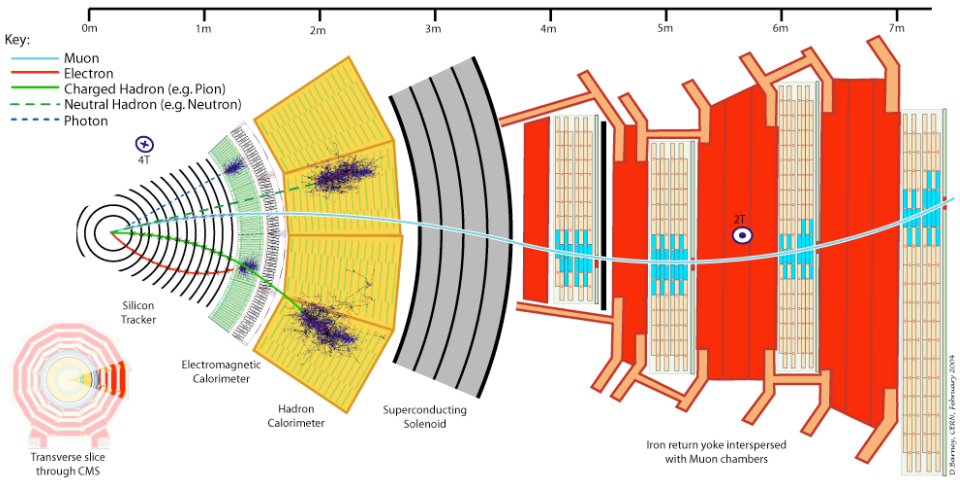

Figure 1: A Schematic of the CMS Detector

VPT Background

At the most basic level, the VPTs are enlisted to take the input scintillation light from the lead tungstate and turn it into a measurable voltage. Because lead tungstate is a fairly weak scintillator (with 1MeV of energy producing approximately 50 photons), the VPTs must provide internal gain. In addition, because the endcap regions can be expected to have radiation doses as high as 200 kGy over a 10 year period, they must be rad-hard. Finally, an energy resolution of less than 1% for photons with energy 100 GeV is required to detect the Higgs boson decay into two photons.

The basic design of the VPT is drawn schematically in Figure 2. A VPT is a single-stage photomultiplier, having a grid for an anode. The reason for the grid can be seen by studying Figure 2; electrons are liberated from the photocathode, and must pass through the anode to first hit the dynode. They will then liberate secondary electrons, and fall back towards the anode. To encourage the electrons along, the anode is maintained at 1000V and the dynode at 800V. VPTs maintain their performance in high magnetic fields largely due to their being single-staged; in multi-staged PMTs secondary electrons would be deflected by the field out of their intended paths, preventing the cascade that is necessary for detection. In addition, having a single-stage with only a limited distance separating the anode and dynode allows for a faster response time for the VPT, an essential quality when the beam is operating at 40 MHz [1].

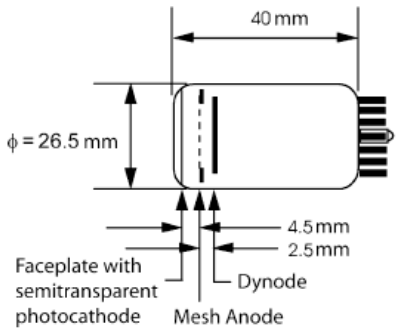

Fig. 2. Diagram of a vacuum phototriode.

While the VPTs have a lot of positives that make them a good fit for ECAL, thre remains the problem of their gain instability. It was observed relatively early on that the gains fluctuated based on a number of parameters. Here, several of the important gain-affecting parameters will be discussed. First, there appears to be a shift in gain, specifically, a move to lower gain, as a function of time since the VPT began to be pulsed by a laser. In other words, as the VPT is consistently pulsed with a laser, the gain lowers in time. Each VPT behaves uniquely; however, the majority are relatively close to one another with a few deviating by as much as 25%. Figures 3 and 4 demonstrate this effect. A subset of VPTs were tested using PN diodes as a controlled measure of the light reaching each VPT. Thus, the VPT voltage was divided by the corresponding PN voltage to get an understanding of how the gain fluctuated with time (the PN gain should remain constant). Figure 3 plots this normalized gain as a function of time for several VPTs

where there was no pulse. Note a present but small change in gain with time. Figure 4 again shows the normalized gain as a function of time, this time with the pulser on. Note the dramatic drop in gain experienced by some VPTs. Figure 5 shows just those VPTs from Figure 4 that experience significant gain drop, as well as information about what the pulser is doing at what time. It should be noted that higher pulse frequencies, in general, correspond to larger drops in gain, and those VPTs that experience a large drop in gain once are most likely to be those that experience a larger drop at a later point (when the pulsing is resumed).

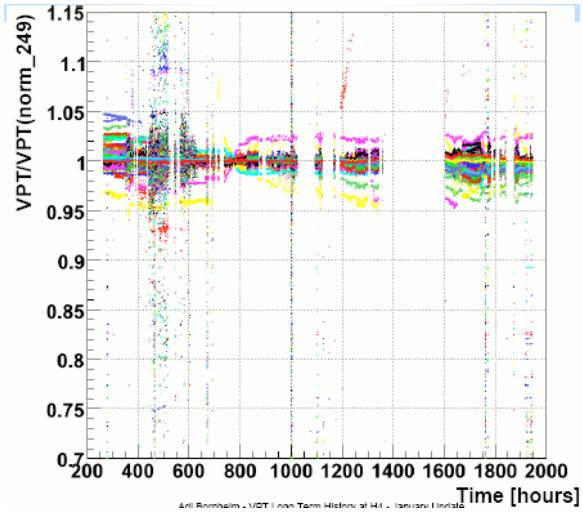

Figure 3: No Pulse

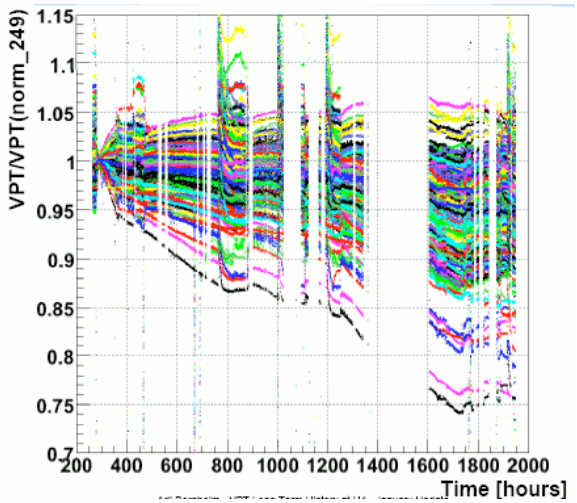

Figure 4: Pulse on

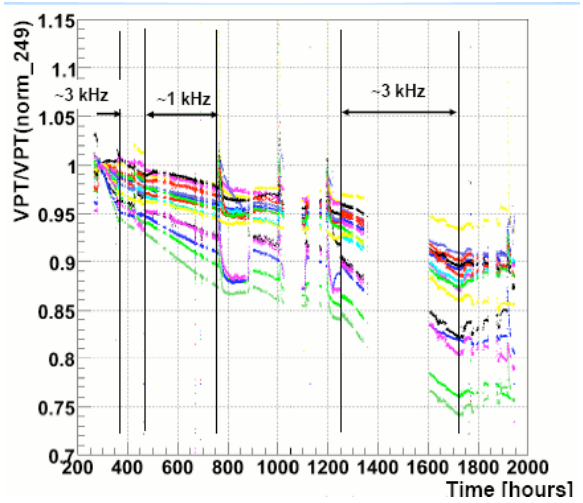

Figure 5: Pulse on; subset of bad VPTs

Figure 6 shows two important effects. First, note that when the frequency of the pulser is reduced, there is an instantaneous increase in gain. Second, note that when pulsing is stopped all together, the gain slowly shifts to a value lower than it began (at T=0, not shown on Figure 6, see Figures 3-5). This is called the classic VPT effect. To summarize the effect, when pulsing is ceased the gain will change with time, and when

pulsing is resumed, the gain will be at a new, somewhat unpredictable value. Note that when pulsing resumed once more (at T=2050 hrs), the gain again drops. Figure 7 highlights two points in time where the pulser was turned on after being off for some time. The interesting point is that the drop in gain over the no-pulse gap was, in general, smaller for the VPTs later in the study. This effect is called burn in. It is thought (or perhaps, hoped) that burn in eventually plateaus, and that it can be cured simply by applying a predefined amount of light for a given amount of time to each VPT before use in the ECAL. However, it is not yet clear if burn in is permanent, or if it, too, fades with time [2].

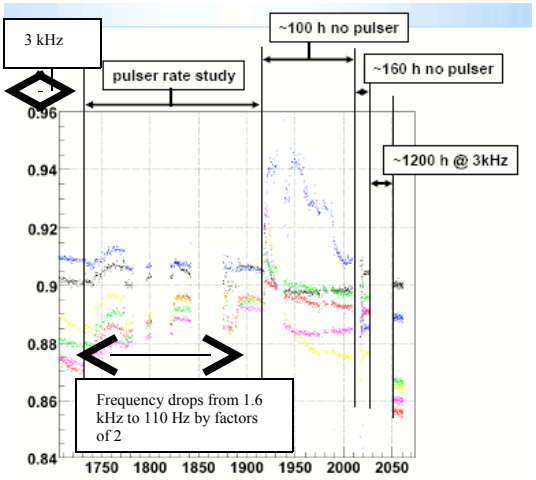

Figure 6: Classic VPT Effect

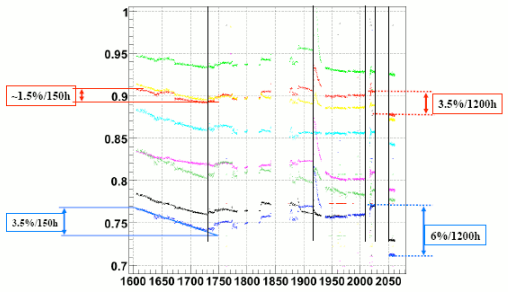

Figure 7: Burn In

In addition to the classic VPT effect and the burn in effect, there is also an effect that has to do with the VPT's angle with the magnetic field. This is an important effect to iron out, because the VPTs will be at varying angles with respect to the magnetic field in the CMS detector. The field angle matters, because the field causes the electrons within the VPT to bend; whether the VPTs are bent perpendicular to the anode or at some angle will affect their collection and subsequent measurement at the anode. Many VPTs were tested in a 1.8 T field, including those shown in Figure 8. However, this is not ideal as they will be used in a 4 T field. Figure 8 shows one VPT's response as a function of angle to a 1.8 T field. Note a smooth change with field.

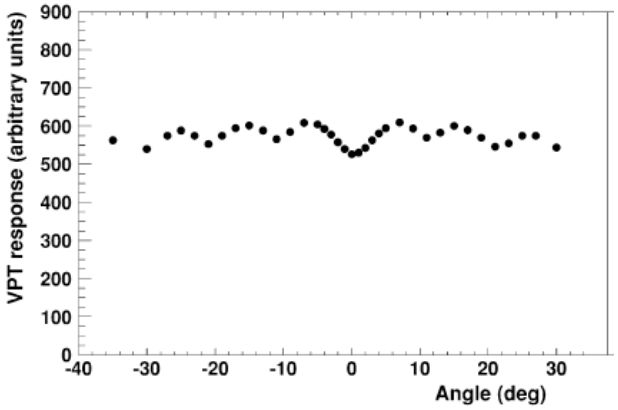

Figure 8: Amplitude as a function of angle, 1.8 T field [1]

However, this is not as severe an effect as some have measured. In many cases, there is what is called the anomalous behavior of VPTs, where at particular angles their "resolution" greatly changes. Here, resolution is taken to mean peak size / peak width. Figure 9 shows a graph of one such VPT's resolution as a function of angle in a 4 T magnetic field. Note the comparison to 0T field. It is planned that those VPTs with high noise will be omitted from the detector, mandated that each VPT be tested before use.

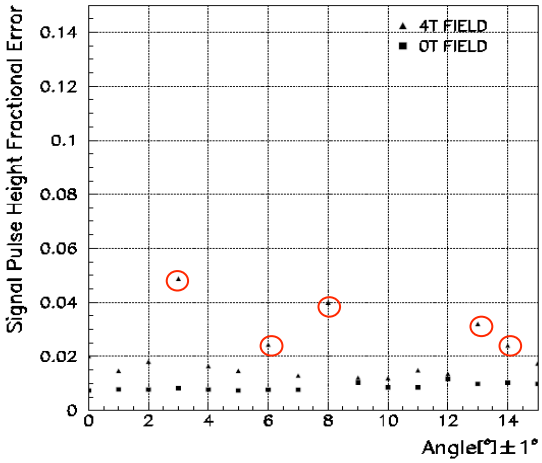

Figure 9: Anomalous VPT Effect[3]

To further study this effect (and any others that may crop up in high field), UVA has obtained a magnet capable of reaching the 4 T mark. With this magnet, it is possible to test a large number of VPTs to better characterize the high-field behavior. The first task was simple but time-consuming.

VPT Pulse Shape in High Field

At various angles to the field, 100 pulsing events were collected for a VPT. A pulsing event was a single input pulse from an LED (held constant throughout the test), with the output voltage of the VPT measured every nanosecond for 1000 ns. Because the output pulse is typically only a few hundred nanoseconds wide, this allowed for a good measure of the pedestal. The VPT output pulse is described by:

$$A(t) = A_0\left(\frac{t-t_0}{\beta}\right)^{\alpha} e^{-\alpha\left(\frac{t-t_0+\beta}{\beta}\right)}, \quad [4]$$

Here A_0 is the overall amplitude, t_0 is the time when the pulse begins, β is the electronics decay time, and the product $\alpha\beta$ is the electronics rise time. To better understand how the field affects the VPT output voltage pulse, a profile according to the above equation was fit to each event, and the constants solved for. In addition to A_0, α, β, and t_0, the pedestal, or the amount of background voltage present without a pulse, was also solved for. Thus, there were five parameters to the fit. These parameters were retained for each of the 100 events at each angle, allowing the shape of the VPT pulse to be tracked as a function of angle.

To facilitate fitting the data, each X and Y pair (time and voltage) were placed into a histogram. Because no fit is robust without some idea of the error on a data point, the approximate error of the data points needed to be calculated. This was done by observing that the last few hundred data points of each event were entirely pedestal, as the pulse had already decayed to background. Thus, by calculating the standard deviation of this background noise, we were able to get an idea of the intrinsic errors in our measurements. To ensure that the pulse was not contributing at all, only the last 100 points were used. This error was then applied to each data point in the fit.

It was also necessary to start the fit with reasonable assumptions of the parameters, lest the fit go off course and crash. The pedestal is perhaps the most intuitive to estimate; the same 100 points used to calculate the standard deviation were averaged to find a good estimate of the pedestal value. The amplitude, A0 was estimated by integrating the entire pulse, or finding its area, and dividing by four. Here, the number four holds no significance, it was determined directly from the data by observing that the amplitude was typically close to ¼ the integral. The time of pulse start, t0, was determined by first finding the location in time of the maximum of the peak, and then subtracting off 45 nanoseconds. Here, again, 45 was determined directly from the data set and holds no significance. Finally, β was assigned the value of 45, and α assigned the value of 1.7. These numbers will be unique to each electronic setup; the average values given in [4] were α= 1.41 and β=39.25ns. It should be noted that our values lie close to these suggested averages. With reasonable starting parameters for our function, the fit was carried out, and the true values of the parameters recorded. Figure 10 shows an example output of the code. The black line represents the raw data points; the blue line is the fit to the data. The upper right corner shows the parameters for the fit, along with some useful information such as the chi squared value and the number of entries.

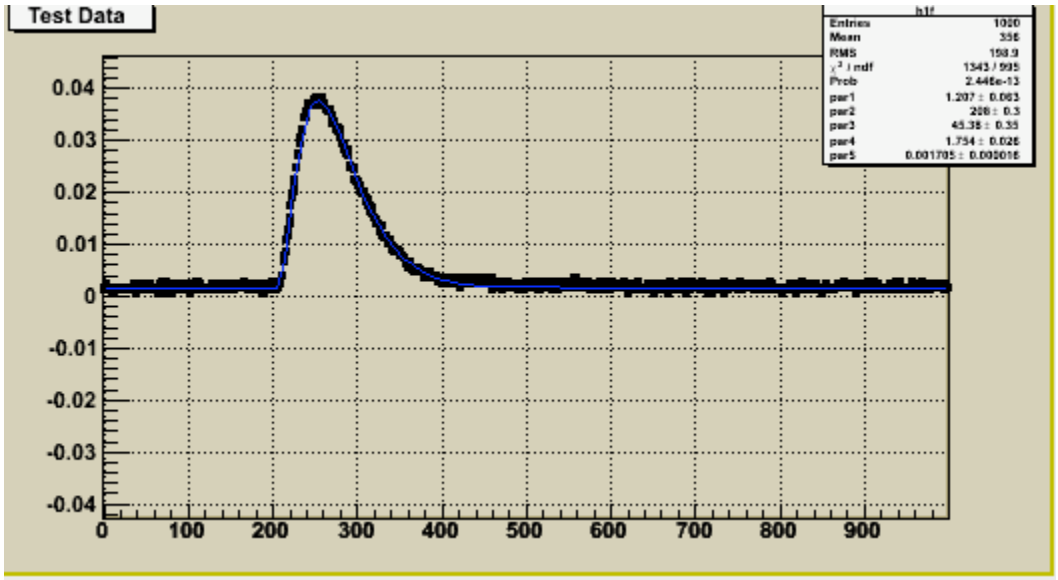

Figure 10: Output of Code; Fitting to VPT Pulse

This is just one event, however. One hundred events were collected for each angle, allowing plots to be made at each angle showing how the various parameters changed within an angle as well as compared to other angles. See Figure 11 for an example of these plots for one angle.

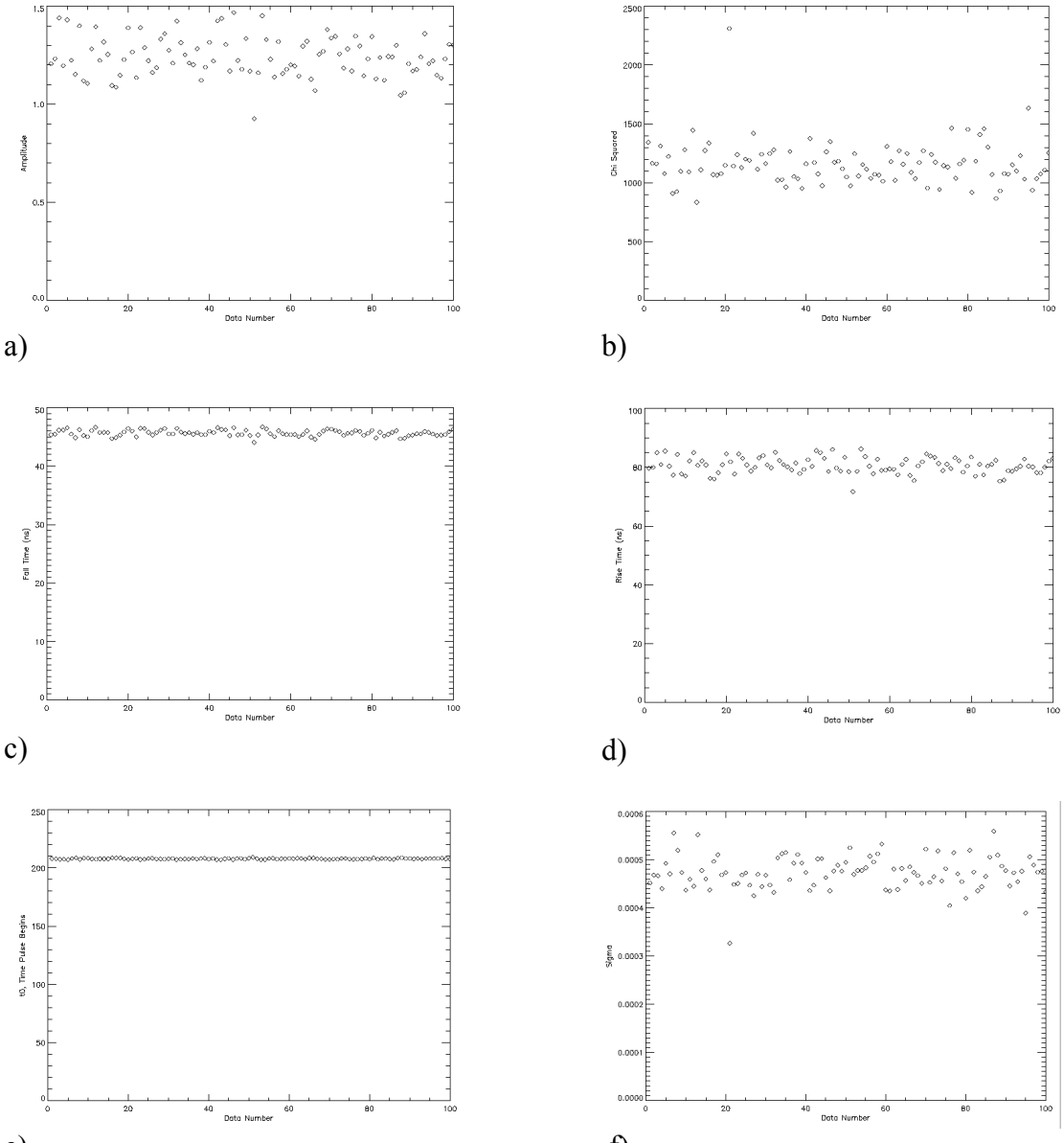

Figure 11: a) Amplitude, b) Chi Squared, c) Fall Time, d) Rise Time, e) T_0, f) Sigma

Notice how consistent t_0 is compared to the other parameters. This is because the same input pulse is used for each event. The amplitudes vary quite a bit, as do the standard deviation of the background. The rise and fall times are relatively consistent throughout.

After analyzing the data for each angle, it was clear that the *shape* of the VPT output pulse was not changing significantly. This is important, because it allows a much easier

method to be used successfully. Instead of fitting a function to each pulse and recording the parameters, the integral of the pulse is recorded, and nothing more. This is a much quicker process, as the integral can be done at the circuit level by charging up a capacitor throughout the length of a pulse, and then reading the voltage across the plates. Assuming that the shape of the pulse is consistent, the integral is all the information you need. Of course the shape varies slightly, but as can be seen from the above plots, the largest fluctuations are seen in the amplitude, which is taken into account in the integral.

VPT at Angles to the Field

With a more rapid approach in hand, it became possible to use more events per angle and test many more VPTs. This was done by taking 5000 events at each angle (-27 degrees through 27 degrees). To switch between negative angles and positive angles, the VPTs were rotated in their boxes inside the magnetic field by 180 degrees, effectively reversing the sign on the angle. Optical fibers carried the light from the LED light source to the VPTs. Data was collected for two different VPTs at a time, as well as a PIN diode, to be used to calibrate the data. The PIN is divided into each VPT pulse, so that any change in light falling on the VPT is divided out, leaving only true VPT effects behind. It is observed that there are smooth changes with angle as well as abrupt changes, similar to the previously mentioned anomalous VPT effect. See Figure 12 for an example of this happening. The red and black diamonds represent two VPTs that were being measured at the same time. Not only is the shape of this curve curious, but the dip at 21 degrees is indicative of the anomalous VPT effect. This dip was not observed in the PIN diode, only in the VPTs, making it a true VPT phenomenon.

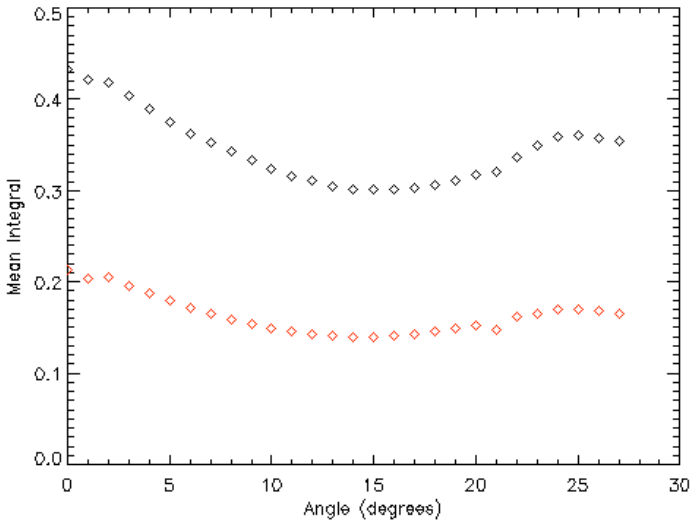

Figure 12: Mean Integral vs Angle

Once the effect of angle on the gain of VPTs is fully understood, the information can be applied to their calibration once in place in the CMS detector. As each VPT will have a constant angle with the field, the effect of the field on the VPT can be divided out.

While the above effect is a fairly minor example of the anomalous VPT effect, as more data is accumulated, surely more VPT mannerisms will crop up. With this testing facility, poorly performing VPTs will be prevented from being incorporated in the detector, and long term stability will be tested.

References

1. Bell, K. W., Brown, R. M., IEEE, 2004.
2. Yohay, Rachel, Powerpoint Slides, 2007
3. Kennedy, B. W., Rutherford Appleton Laboratory, 2002.
4. Anfrevilleb, M., Bailleuxa, D. et. Al, CMS Note -2007/028, 2006.